NANO LETTERS
Letter
Cite This: Nano Lett. 2020, 20, 553−558
pubs.acs.org/NanoLett

Coexistence of Magnetic Orders in Two-Dimensional Magnet CrI_3

Ben Niu,[†,‡,▽] Tang Su,[§,‡,▽] Brian A. Francisco,[‡] Subhajit Ghosh,[∥] Fariborz Kargar,[∥] Xiong Huang,[⊥] Mark Lohmann,[‡] Junxue Li,[‡] Yadong Xu,[‡] Takashi Taniguchi,[#] Kenji Watanabe,[#] Di Wu,[†] Alexander Balandin,[∥] Jing Shi,[*,‡] and Yong-Tao Cui[*,‡]

[†]National Laboratory of Solid State Microstructures, Department of Materials Science and Engineering, Jiangsu Key Laboratory for Artificial Functional Materials, and Collaborative Innovation Center of Advanced Microstructures, Nanjing University, Nanjing 210093, China

[‡]Department of Physics and Astronomy, University of California, Riverside, California 92521, United States

[§]International Center for Quantum Materials, School of Physics, Peking University, Beijing 100871, P.R. China

[∥]Department of Electrical and Computer Engineering and [⊥]Department of Materials Science and Engineering, University of California, Riverside, California 92521, United States

[#]National Institute for Materials Science, 1-1 Namiki, Tsukuba, 305-0044, Japan

Supporting Information

ABSTRACT: The magnetic properties in two-dimensional van der Waals materials depend sensitively on structure. CrI_3, as an example, has been recently demonstrated to exhibit distinct magnetic properties depending on the layer thickness and stacking order. Bulk CrI_3 is ferromagnetic (FM) with a Curie temperature of 61 K and a rhombohedral layer stacking, whereas few-layer CrI_3 has a layered antiferromagnetic (AFM) phase with a lower ordering temperature of 45 K and a monoclinic stacking. In this work, we use cryogenic magnetic force microscopy to investigate CrI_3 flakes in the intermediate thickness range (25−200 nm) and find that the two types of magnetic orders, hence the stacking orders, can coexist in the same flake with a layer of ∼13 nm at each surface being in the layered AFM phase similar to few-layer CrI_3 and the rest in the bulk FM phase. The switching of the bulk moment proceeds through a remnant state with nearly compensated magnetic moment along the *c*-axis, indicating formation of *c*-axis domains allowed by a weak interlayer coupling strength in the rhombohedral phase. Our results provide a comprehensive picture on the magnetism in CrI_3 and point to the possibility of engineering magnetic heterostructures within the same material.

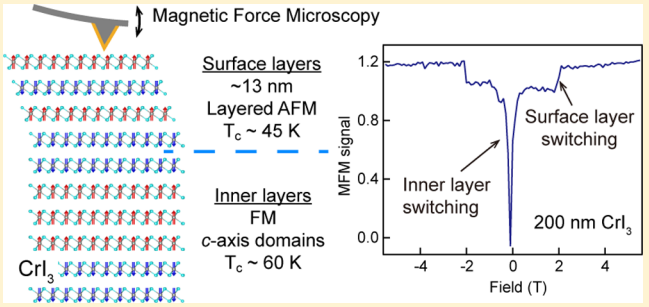

KEYWORDS: *Magnetic force microscopy, 2D magnets, CrI_3, magnetic orders, magnetization switching*

The recent discoveries of intrinsic magnetism in several van der Waals (vdW) materials[1,2] have generated widespread interest in the study of magnetism in two dimensions,[3−5] as their vdW nature allows exfoliation of thin flakes down to the monolayer limit. These two-dimensional (2D) magnetic systems exhibit exciting magnetic, electrical, and optical properties, such as giant tunneling magnetoresistance,[6−9] magnetoelectric coupling,[10−12] and magnetic second harmonic generation,[13] promising for future spintronics applications. Meanwhile, several important questions regarding their magnetic properties in both bulk crystals and few layer flakes remain elusive. In bulk CrI_3 crystal, previous magnetic characterizations indicate a ferromagnetic order with a *c*-axis anisotropy and a small (<0.2 T) magnetic field is able to saturate the magnetization along the *c*-axis.[14,15] However, the magnetization versus field (M-H) loop shows little hysteresis and a very small remnant magnetization at zero field, which was explained by the formation of magnetic domains in bulk crystals, but has yet to be confirmed.[14] On the other hand, exfoliated CrI_3 flakes in the few-layer limit show distinct magnetic properties from the bulk. Few layer CrI_3 is found to be a layered antiferromagnet with a Curie temperature of ∼45 K compared to the bulk T_c of ∼61 K.[1,8,9,16] It also requires a much larger magnetic field (∼1−2 T) to reverse individual layers to polarize the magnetization.[1,6−9] Recent experimental[13,17−19] and theoretical[20−23] studies have suggested that the difference in the magnetic order originates from different layer stacking orders: bulk CrI_3 undergoes a structural phase transition from its high-temperature monoclinic phase to a rhombohedral phase at ∼200 K, but this transition is suppressed in exfoliated few-layer CrI_3 so that it remains in the monoclinic phase at low temperatures with a different magnetic configuration. It is thus interesting to examine over what thickness range the layer stacking order recovers to the

Received: October 17, 2019
Revised: November 16, 2019
Published: November 26, 2019

DOI: 10.1021/acs.nanolett.9b04282
Nano Lett. 2020, 20, 553−558

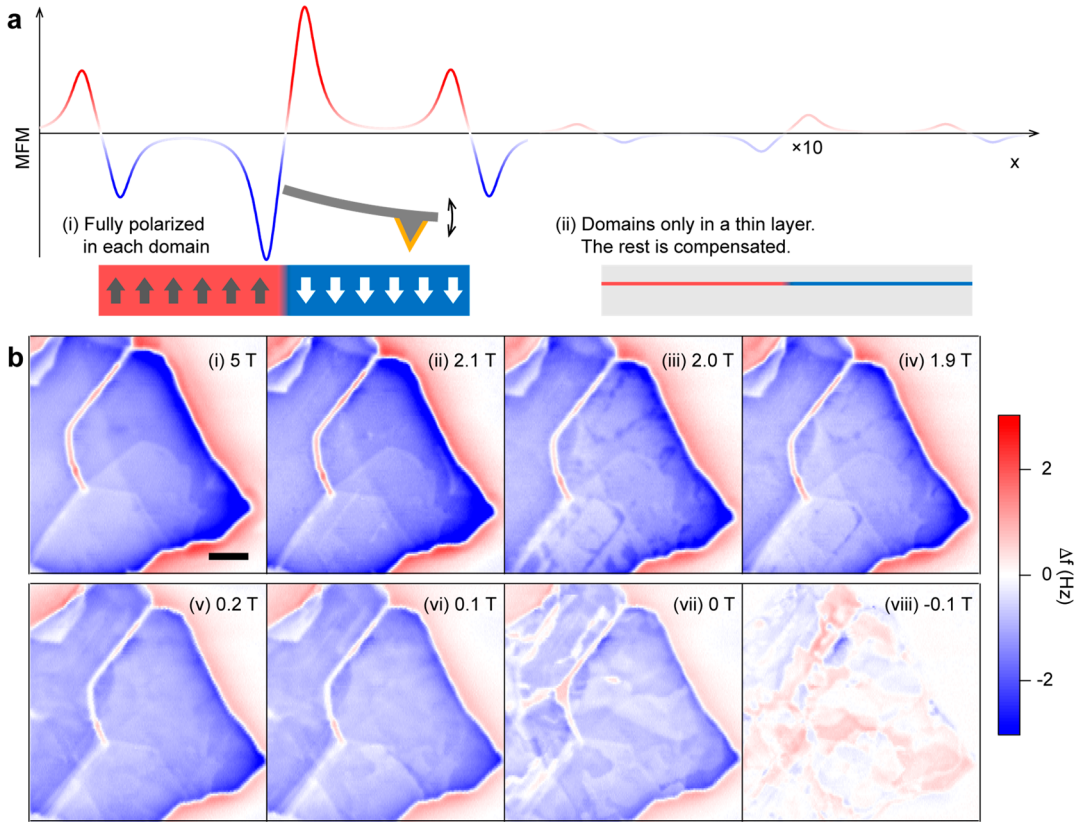

Figure 1. MFM imaging of the magnetic switching in exfoliated CrI_3. (a) Simulated MFM signal across magnetic domains in two scenarios: (i) Moments are fully polarized in each domain. (ii) Domains only exist in a thin layer with zero net moment in rest of the sample. The MFM signal in (ii) is scaled by a factor of 10. (b) MFM images of a 200 nm CrI_3 flake with magnetic field decreasing from 5 T to −0.1 T. Scale bar is 2 μm.

bulk phase. To address these questions, we perform cryogenic magnetic force microscopy to study the magnetic properties in thin CrI_3 flakes of various thicknesses. We find that the two types of magnetic configurations coexist in thin CrI_3 flakes: surface layers of ∼13 nm exhibit an AFM interlayer coupling similar to exfoliated few-layer CrI_3 in the monoclinic phase, whereas the inner layers behave similarly to CrI_3 bulk crystals with a FM interlayer coupling which is weaker in strength than that of the AFM coupling in the surface layers, resulting in a remnant state with nearly compensated magnetic moment along the *c*-axis.

In our experiment, thin CrI_3 flakes were prepared by mechanical exfoliation and covered by hexagonal boron nitride (hBN) flakes in an inert environment to minimize CrI_3 degradation. (See more details in Supporting Information (SI).) Magnetic force microscopy was performed in a cryogenic environment with a magnetic field applied perpendicular to CrI_3 flakes. In magnetic force microscopy (MFM) measurement, a cantilever probe coated with a thin magnetic film was used to sense the force exerted by the sample's magnetic fields on the probe. Specifically, the change in the probe's mechanical resonant frequency is proportional to the spatial derivative of the magnetic field. Therefore, MFM is highly sensitive to the formation of lateral magnetic domains in which domain walls produce strong spatial variations of magnetic fields but a laterally uniform magnetization also produces a finite but smaller MFM signal as the magnetic field decays away from the sample surface, as illustrated by a simulated MFM curve shown in Figure 1a. In the latter case, the MFM signal is proportional to the areal density of the sample moment integrated over the thickness dimension, which can be used as a nanoscale magnetometer to measure the local magnetization strength.

First, we examine the magnetic configuration during the reversal process in a 200 nm CrI_3 flake. Figure 1b shows representative MFM images of this flake at different magnetic fields. At B = 5 T, where the magnetization is fully aligned, the sample shows a roughly uniform MFM signal inside the flake which only has strong variations near the CrI_3 edge due to the geometry of the stray field. The negative sign of the MFM signals in the interior of the flake indicates an attractive force because the moments of both sample and probe are aligned along the same direction by the applied magnetic field. The weak contrast pattern in the interior corresponds to regions of different thicknesses hence different magnetic moments. (See SI for a comparison with the sample topography.) The roughly uniform configuration persists as the field is reduced all the way to around 0.2 T, except within a narrow field range between 2.1 and 1.9 T where magnetic domains appear. But the MFM signal inside the bulk only changes slightly through this range, indicating a partial reversal of the moments. Until about 0.2 T, the average MFM signal in the bulk starts to change quickly, and domains with weak contrasts appear and evolve continuously as the field is further reduced. Around −0.1 T, the average signal reaches around 0 whereas the signal contrast across domains remains weak. When the field is further reduced below −0.1 T through −5 T, the MFM signal follows an evolution similar to the positive field side. (See SI for more MFM images.) Such a weak MFM signal pattern suggests that although domains form during the reversal

DOI: 10.1021/acs.nanolett.9b04282
Nano Lett. 2020, 20, 553−558

process, the thickness-integrated areal density of moments in individual domains are small, similar to the simulated case in Figure 1a (ii). In the remnant state, the total moment is nearly compensated along the *c*-axis.

Next, we study more quantitatively the change in magnetic moment during the reversal process and demonstrate that two types of magnetic configurations coexist in CrI_3 flakes. The MFM images suggest that the magnetic configuration during most of the reversal process is spatially uniform. In this case, the MFM signal will be roughly proportional to the areal density of magnetic moment integrated over the flake thickness. On the basis of this property, we measure the MFM signal inside the flake as a function of magnetic field, as shown in Figure 2a. (Note that we plot $-\Delta f$ to represent the magnitude of the magnetic moment where the negative sign accounts for the attractive nature of the magnetic force.) The MFM versus *B* curve captures the switching process as the magnetic moment is fully reversed, which exhibits two distinct stages as hinted already by the MFM images. When sweeping down from the fully polarized state at 5 T, the MFM signal remains roughly constant until around 2 T where it decreases by a step over a small field range. It then again remains roughly constant until about 0.2 T. Below 0.2 T, the signal quickly decreases to zero at −0.1 T. After the field is further swept to negative values, the behavior of the MFM signal is similar to the positive field side: the magnetization is reversed along the opposite direction in two stages. (Note that the moment of the MFM tip is also reversed at negative field, so the sign of the MFM signal remains the same.) The two stages of the switching process suggest that this 200 nm CrI_3 flake can be divided into two groups of layers with different magnetic properties. One group has its switching field at ∼2 T (referred to below as "hard layers"), which is very similar to the switching properties in few-layer CrI_3. In contrast, the other group of "soft layers" switches at low field, similar to the soft switching behavior seen in CrI_3 bulk crystals. From the relative ratio of the signal changes for these two groups, we calculate the effective thickness of each group: the hard layers contribute ∼12% of the full-scale signal which converts to ∼24 nm in thickness, and the soft layers span the rest. This behavior of two-stage switching is quite general in flakes of different thicknesses. In all flakes that we have measured, there always exists one group of hard layers that switch at ∼2 T. (See Figure 2b,c and more examples in SI.) The relative percentage of this group increases as the flake thickness decreases but the calculated effective thickness is roughly a constant around 25 nm which varies slightly in different samples (Figure 2d). In the 25 nm flake, all the moments switch together at ∼2 T, and no soft layers can be identified. This thickness dependence can be explained because the hard layers correspond to the surface layers of the CrI_3 flake whereas the soft layers correspond to the inner layers. As the total thickness decreases, the thickness of the hard surface layers remains constant whereas the soft

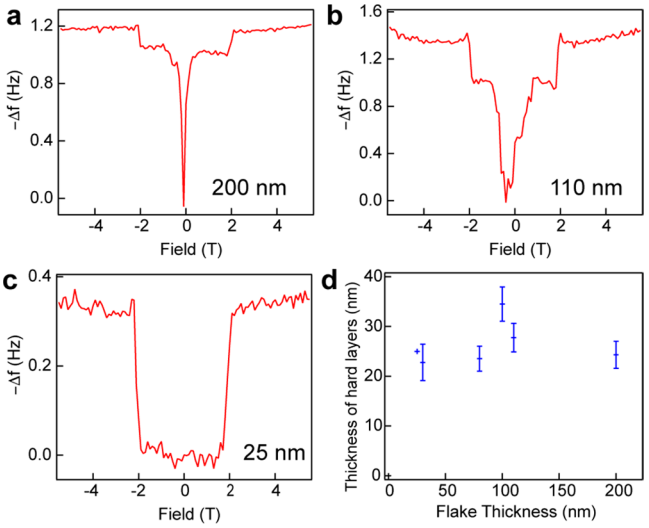

Figure 2. Two groups of layers with different magnetic properties coexist in CrI_3 flakes. (a−c) MFM signal as a function of magnetic field for three flakes with thicknesses of (a) 200, (b) 110, and (c) 25 nm. (d) Calculated thicknesses of the hard layers in CrI_3 flakes with thicknesses ranging from 25 to 200 nm.

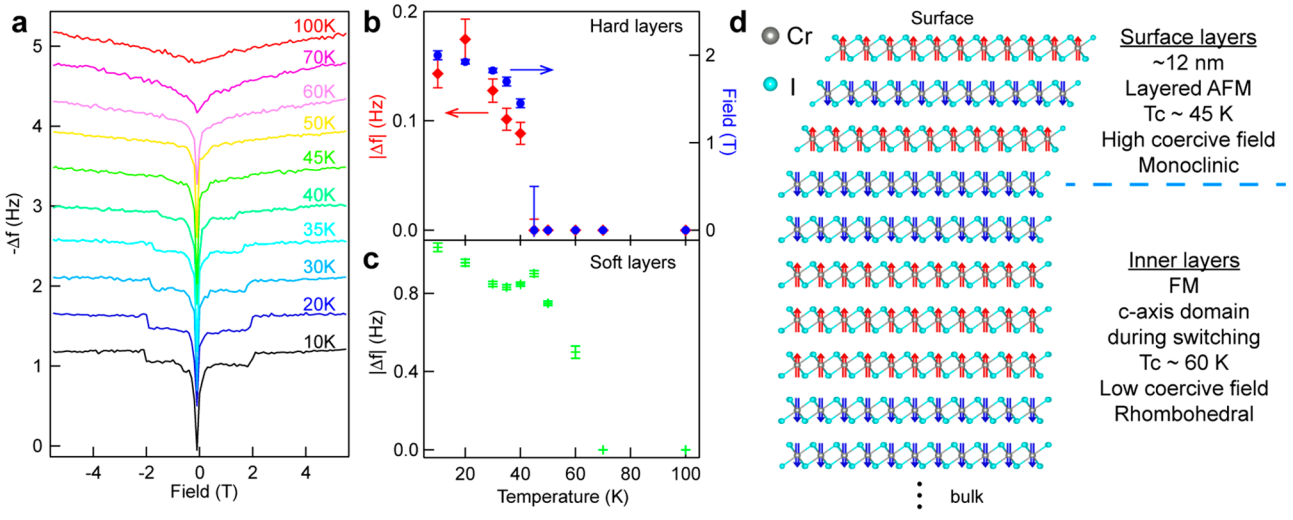

Figure 3. Temperature dependence of MFM signals in the surface and inner layers. (a) MFM versus magnetic field in the 200 nm CrI_3 flake at temperatures from 10 to 100 K. (b) The MFM signal change and the switching field of the hard layer as a function of temperature. (c) The MFM signal associated with the switching of soft layers as a function of temperature. (d) Illustration of the stacking orders and spin configurations in surface and inner layers.

DOI: 10.1021/acs.nanolett.9b04282
Nano Lett. 2020, 20, 553−558

inner layer portion shrinks until the total thickness is below ~25 nm; then the soft inner layer group disappears and the entire flake behaves as one group that switches only at ~2 T. Because every flake always has two surfaces, the hard layers at each surface should have a thickness of ~13 nm.

The hard and soft layers also have different Curie temperatures. Figure 3a plots the MFM signal versus B curves for the 200 nm flake at temperatures from 10 K up to 100 K. As temperature increases, the switching field of the hard layers decreases from 2 T and the associated change in the MFM signal decreases as well. Around 45−50 K, no switching can be identified for this group. Figure 3b plots the temperature dependence of the switching field and the MFM signal change for the hard layers from which we estimate its Curie temperature to be ~45 K, similar to the Curie temperature in few layer CrI_3. In contrast, the soft switching at low field still persists up to 60 K. The size of the signal which reflects the magnetic moment of the soft inner layers decreases with increasing temperature and reaches zero between 60 and 70 K, resembling the behavior in CrI_3 bulk crystal which has a Curie temperature of 61 K.

On the basis of our observations, we present the following picture to describe the magnetic configuration in these CrI_3 flakes, as illustrated in Figure 3d. First, the surface layers have a layered AFM configuration which is similar to that in few-layer CrI_3, that is, ferromagnetically coupled within each layer but antiferromagnetically coupled between adjacent layers.[1] These layers switch from the layered AFM state to the fully polarized FM state at ~2 T, as indicated by the abrupt change in the MFM signal. Second, during the switching of the inner layers at low fields, the gradual decrease of the MFM signal and the lack of strong domain contrasts suggests that the inner layers switch layer by layer where the weak lateral domain contrasts indicate the formation of lateral domains within the individual layer that is undergoing switching. At the remnant state, the CrI_3 flakes have a very small, nearly compensated, residue moment integrated over thickness. These behaviors rule out the possibility of a strong interlayer-coupled FM state, because in that case it will favor a domain switching process where magnetic moments are fully polarized along the c-axis in individual domains but pointing along opposite directions between lateral neighbors, which would generate a strong MFM signal near the domain wall, at least stronger than that of the fully polarized state at high fields,[24] as illustrated in Figure 1a. There could be two possible scenarios: (a) The inner layers have a layered AFM state so that the remnant state has a zero moment. The interlayer AFM coupling in the inner layers should be much weaker than that in the surface layers, therefore the inner layers switch at much lower fields. (b) The inner layers have an FM interlayer coupling but domains form along the c-axis during the switching in order to lower the magnetostatic energy. In this case, the FM-coupled inner layers can still have a nearly compensated moment at remnant. The interlayer FM coupling strength should be very weak to allow a small c-axis domain size, and it also explains that the switching onsets before the applied field reverses direction because of the demagnetization field. In both cases, the magnitudes of the interlayer exchange coupling should be small, whereas our measurements cannot conclusively determine its sign. (See further discussion on the sign below.)

The remaining question now is what causes the magnetic properties in the surface layers to differ from the inner layers. Recent experimental[13,17−19] and theoretical[20−23] studies have uncovered a close relation between the magnetic order and the layer stacking order in CrI_3. Bulk CrI_3 is in a monoclinic phase at room temperature and undergoes a structural phase transition to a rhombohedral phase at around 200 K.[14,25] The main difference between the two phases is different stacking orders of the CrI_3 layers. Second harmonic generation,[13] high pressure,[17,18] and Raman[19] experiments demonstrate that exfoliated few-layer CrI_3 flakes remain in the monoclinic phase at all temperatures. Given the similarity in magnetic properties between the surface layer group in our samples and few-layer CrI_3 flakes, and between the inner layer group and CrI_3 bulk crystals, we believe that the surface layers, which are about ~13 nm thick at each surface, should be in the monoclinic phase at all temperatures like few-layer CrI_3 flakes, whereas the inner layers undergo the structural phase transition like bulk CrI_3. Therefore, the monoclinic surface layers exhibit a layered AFM order with a Curie temperature of 45 K, whereas the rhombohedral inner layers have a higher Curie temperature at around 60−70 K with weaker interlayer coupling strengths. Exfoliated CrI_3 flakes thicker than ~25 nm will have these two phases coexisting, whereas thinner flakes are entirely in the monoclinic phase.

Recent high-pressure measurements[17,18] have demonstrated that few-layer CrI_3 flakes can be switched from the monoclinic to the rhombohedral phase and the magnetic order switches from the layered AFM state to the FM state accordingly. These results suggest that the rhombohedral phase of CrI_3 favors an FM interlayer coupling. Correlating this conclusion with our results supports the proposed scenario (b), that is, the inner layers have a weak FM coupling and their switching at low fields proceeds with formation of c-axis domains.

The mechanism by which the structural phase transition is suppressed in the surface layers of CrI_3 flakes is likely due to surface effect, for example, defects in the surface layer, the interaction between the surface layer and hBN, surface strains created during the mechanical exfoliation process, or simply just having a surface where the interlayer coupling only comes from one side. Our results indicate that such a surface effect can modify the stacking order not only in the topmost few layers but roughly ~13 nm (almost 20 layers) into the bulk. The stacking order in these ~20 layers should be quite uniform as indicated by the sharp switching around 2 T consistent in different samples. The switching of the inner layers exhibits more variations across samples (see, for example, the flakes in Figure 2a,b and more data in SI), which could possibly be due to a transition phase between the two different stacking orders. It would be interesting to investigate how the layer stacking transits from the monoclinic to the rhombohedral phase across their interface. The correlation between magnetic order and layer stacking has also been found in two other chromium trihalides, $CrBr_3$[26] and $CrCl_3$,[27] so multiple structure phases and magnetic orders could also coexist in their exfoliated flakes. The coexistence of the two magnetic configurations naturally forms a magnetic heterostructure within the same material but with drastically different magnetic properties, the AFM phase at two surfaces and the FM phase in the interior layers. Further studies on the electronic properties across such sandwich structure could potentially realize new device functionalities, and developing methods to control the transition and thickness of the two phases would provide new opportunities to engineer magnetic states in these van der Waals materials and new insights on the magnetism in two dimensions.

DOI: 10.1021/acs.nanolett.9b04282
Nano Lett. 2020, 20, 553−558

Methods. CrI_3 flakes were mechanically exfoliated in an Ar-filled glovebox and a dry transfer method is used to form a sandwich structure where CrI_3 is protected by thin hBN flakes on both sides. (See further fabrication details in SI.) Magnetic force microscopy measurement was performed on a home-built cryogenic scanning probe platform. Commercial MFM probes with Co—Cr coating and a nominal coercivity of 400 Oe were used. In MFM measurement, the probe was scanned over the sample surface at a constant height of ∼100−150 nm. The MFM signal, that is, the change in the cantilever resonant frequency, was measured using a phase locked loop. During scanning, a potential feedback loop similar to that in an electrostatic force microscope was used to apply a tip bias to compensate the tip−sample potential difference in order to minimize the electrostatic force on the probe. More details on the potential compensation are provided in SI.

■ ASSOCIATED CONTENT

Supporting Information

The Supporting Information is available free of charge at https://pubs.acs.org/doi/10.1021/acs.nanolett.9b04282.

Sample fabrication, experimental setup, MFM images during the magnetic field sweep, determination of the hard layer thickness, thickness dependence, temperature dependence (PDF)

■ AUTHOR INFORMATION

Corresponding Authors

*E-mail: jing.shi@ucr.edu.
*E-mail: yongtao.cui@ucr.edu.

ORCID

Fariborz Kargar: 0000-0003-2192-2023
Di Wu: 0000-0003-3619-1411
Jing Shi: 0000-0002-9395-8482
Yong-Tao Cui: 0000-0002-8015-1049

Author Contributions

Y.T.C. and J.S. initiated and supervised the project. B.N. performed the MFM measurements with assistance from X.H. and B.A.F. T.S. fabricated the device with help from M.L., J.X.L., and Y.X. B.A.F. performed MFM simulations. S.G. and F.K. carried out the Raman characterization under supervision of A.B. D.W. provided support for the visit by B.N. to UCR. T.T. and K.W. provided hBN crystals. B.N., T.S., J.S., and Y.T.C analyzed the data and wrote the paper with comments from all authors.

Author Contributions

$^{\nabla}$B.N. and T.S. contributed equally to this work.

Notes

The authors declare no competing financial interest.

■ ACKNOWLEDGMENTS

We thank Kin Fai Mak, Jie Shan, and Liuyan Zhao for helpful discussions. The MFM work was supported by the start-up funds from the Regents of the University of California. T.S., J.X.L., M.L., and J.S. acknowledge support from DOE BES Grant DE-FG02-07ER46351. B.N. and D.W. acknowledge support from the Natural Science Foundation of China (51725203, 51721001, and U1932115). Visits by B.N. and T.S. at UCR were supported by the China Scholarship Council (CSC). K.W. and T.T. acknowledge support from the Elemental Strategy Initiative conducted by the MEXT, Japan and the CREST (JPMJCR15F3), JST.

■ REFERENCES

(1) Huang, B.; Clark, G.; Navarro-Moratalla, E.; Klein, D. R.; Cheng, R.; Seyler, K. L.; Zhong, D.; Schmidgall, E.; McGuire, M. A.; Cobden, D. H.; Yao, W.; Xiao, D.; Jarillo-Herrero, P.; Xu, X. Layer-dependent ferromagnetism in a van der Waals crystal down to the monolayer limit. *Nature* **2017**, *546*, 270−273.

(2) Gong, C.; Li, L.; Li, Z.; Ji, H.; Stern, A.; Xia, Y.; Cao, T.; Bao, W.; Wang, C.; Wang, Y.; Qiu, Z. Q.; Cava, R. J.; Louie, S. G.; Xia, J.; Zhang, X. Discovery of intrinsic ferromagnetism in two-dimensional van der Waals crystals. *Nature* **2017**, *546*, 265−269.

(3) Gong, C.; Zhang, X. Two-dimensional magnetic crystals and emergent heterostructure devices. *Science* **2019**, *363*, No. eaav4450.

(4) Burch, K. S.; Mandrus, D.; Park, J.-G. Magnetism in two-dimensional van der Waals materials. *Nature* **2018**, *563*, 47−52.

(5) Gibertini, M.; Koperski, M.; Morpurgo, A. F.; Novoselov, K. S. Magnetic 2D materials and heterostructures. *Nat. Nanotechnol.* **2019**, *14*, 408−419.

(6) Song, T.; Cai, X.; Tu, M. W.-Y.; Zhang, X.; Huang, B.; Wilson, N. P.; Seyler, K. L.; Zhu, L.; Taniguchi, T.; Watanabe, K.; McGuire, M. A.; Cobden, D. H.; Xiao, D.; Yao, W.; Xu, X. Giant tunneling magnetoresistance in spin-filter van der Waals heterostructures. *Science* **2018**, *360*, 1214−1218.

(7) Klein, D. R.; MacNeill, D.; Lado, J. L.; Soriano, D.; Navarro-Moratalla, E.; Watanabe, K.; Taniguchi, T.; Manni, S.; Canfield, P.; Fernández-Rossier, J.; Jarillo-Herrero, P. Probing magnetism in 2D van der Waals crystalline insulators via electron tunneling. *Science* **2018**, *360*, 1218−1222.

(8) Wang, Z.; Gutiérrez-Lezama, I.; Ubrig, N.; Kroner, M.; Gibertini, M.; Taniguchi, T.; Watanabe, K.; Imamoğlu, A.; Giannini, E.; Morpurgo, A. F. Very large tunneling magnetoresistance in layered magnetic semiconductor CrI3. *Nat. Commun.* **2018**, *9*, 2516.

(9) Kim, H. H.; Yang, B.; Patel, T.; Sfigakis, F.; Li, C.; Tian, S.; Lei, H.; Tsen, A. W. One Million Percent Tunnel Magnetoresistance in a Magnetic van der Waals Heterostructure. *Nano Lett.* **2018**, *18*, 4885−4890.

(10) Wang, Z.; Zhang, T.; Ding, M.; Dong, B.; Li, Y.; Chen, M.; Li, X.; Huang, J.; Wang, H.; Zhao, X.; Li, Y.; Li, D.; Jia, C.-K.; Sun, L.; Guo, H.; Ye, Y.; Sun, D.-M.; Chen, Y.-S.; Yang, T.; Zhang, J.; Ono, S.; Han, Z.; Zhang, Z.-D. Electric-field control of magnetism in a few-layered van der Waals ferromagnetic semiconductor. *Nat. Nanotechnol.* **2018**, *13*, 554−559.

(11) Jiang, S.; Shan, J.; Mak, K. F. Electric-field switching of two-dimensional van der Waals magnets. *Nat. Mater.* **2018**, *17*, 406−410.

(12) Jiang, S.; Li, L.; Wang, Z.; Mak, K. F.; Shan, J. Controlling magnetism in 2D CrI3 by electrostatic doping. *Nat. Nanotechnol.* **2018**, *13*, 549−553.

(13) Sun, Z.; Yi, Y.; Song, T.; Clark, G.; Huang, B.; Shan, Y.; Wu, S. S.; Huang, D.; Gao, C.; Chen, Z.; McGuire, M.; Cao, T.; Xiao, D.; Liu, W.-T.; Yao, W.; Xu, X.; Wu, S. S. Giant and nonreciprocal second harmonic generation from layered antiferromagnetism in bilayer CrI3. *Nature* **2019**, *572*, 497.

(14) McGuire, M. A.; Dixit, H.; Cooper, V. R.; Sales, B. C. Coupling of Crystal Structure and Magnetism in the Layered, Ferromagnetic Insulator CrI3. *Chem. Mater.* **2015**, *27*, 612−620.

(15) Liu, Y.; Wu, L.; Tong, X.; Li, J.; Tao, J.; Zhu, Y.; Petrovic, C. Thickness-dependent magnetic order in CrI3 single crystals. *Sci. Rep.* **2019**, *9*, 13599.

(16) Thiel, L.; Wang, Z.; Tschudin, M. A.; Rohner, D.; Gutiérrez-Lezama, I.; Ubrig, N.; Gibertini, M.; Giannini, E.; Morpurgo, A. F.; Maletinsky, P. Probing magnetism in 2D materials at the nanoscale with single-spin microscopy. *Science* **2019**, *364*, 973−976.

(17) Song, T.; Fei, Z.; Yankowitz, M.; Lin, Z.; Jiang, Q.; Hwangbo, K.; Zhang, Q.; Sun, B.; Taniguchi, T.; Watanabe, K.; McGuire, M. A.; Graf, D.; Cao, T.; Chu, J.-H.; Cobden, D. H.; Dean, C. R.; Xiao, D.; Xu, X. Switching 2D Magnetic States via Pressure Tuning of Layer Stacking. *Nat. Mater.* **2019**, *18*, 1298.

DOI: 10.1021/acs.nanolett.9b04282
Nano Lett. 2020, 20, 553−558

(18) Li, T.; Jiang, S.; Sivadas, N.; Wang, Z.; Xu, Y.; Weber, D.; Goldberger, J. E.; Watanabe, K.; Taniguchi, T.; Fennie, C. J.; Mak, K. F.; Shan, J. Pressure-controlled interlayer magnetism in atomically thin CrI3. *Nat. Mater.* **2019**, *18*, 1303.
(19) Ubrig, N.; Wang, Z.; Teyssier, J.; Taniguchi, T.; Watanabe, K.; Giannini, E.; Morpurgo, A. F.; Gibertini, M. Low-temperature monoclinic layer stacking in atomically thin CrI3 crystals. *2D Mater.* **2020**, *7*, 015007.
(20) Soriano, D.; Cardoso, C.; Fernández-Rossier, J. Interplay between interlayer exchange and stacking in CrI3 bilayers. *Solid State Commun.* **2019**, *299*, 113662.
(21) Sivadas, N.; Okamoto, S.; Xu, X.; Fennie, C. J.; Xiao, D. Stacking-Dependent Magnetism in Bilayer CrI3. *Nano Lett.* **2018**, *18*, 7658−7664.
(22) Jiang, P.; Wang, C.; Chen, D.; Zhong, Z.; Yuan, Z.; Lu, Z.-Y.; Ji, W. Stacking tunable interlayer magnetism in bilayer CrI3. *Phys. Rev. B: Condens. Matter Mater. Phys.* **2019**, *99*, 144401.
(23) Jang, S. W.; Jeong, M. Y.; Yoon, H.; Ryee, S.; Han, M. J. Microscopic understanding of magnetic interactions in bilayer CrI3. *Phys. Rev. Mater.* **2019**, *3*, 031001.
(24) Lohmann, M.; Su, T.; Niu, B.; Hou, Y.; Alghamdi, M.; Aldosary, M.; Xing, W.; Zhong, J.; Jia, S.; Han, W.; Wu, R.; Cui, Y.; Shi, J. Probing Magnetism in Insulating Cr2Ge2Te6 by Induced Anomalous Hall Effect in Pt. *Nano Lett.* **2019**, *19*, 2397−2403.
(25) Djurdjić-Mijin, S.; Šolajić, A.; Pešić, J.; Šćepanović, M.; Liu, Y.; Baum, A.; Petrovic, C.; Lazarević, N.; Popović, Z. V. Lattice dynamics and phase transition in CrI3 single crystals. *Phys. Rev. B: Condens. Matter Mater. Phys.* **2018**, *98*, 104307.
(26) Chen, W.; Sun, Z.; Gu, L.; Xu, X.; Wu, S.; Gao, C. Direct observation of van der Waals stacking dependent interlayer magnetism. *Science* **2019**, *366*, 983.
(27) Klein, D. R., MacNeill, D., Song, Q., Larson, D. T., Fang, S., Xu, M., Ribeiro, R. A., Canfield, P. C., Kaxiras, E., Comin, R.; Jarillo-Herrero, P. Enhancement of interlayer exchange in an ultrathin two-dimensional magnet. *Nat. Phys.* **2019** DOI: 10.1038/s41567-019-0651-0.

DOI: 10.1021/acs.nanolett.9b04282
Nano Lett. 2020, 20, 553−558